

Supporting Information

Photovoltaic Effects of the CdS and PbS Quantum Dots Encapsulated in Zeolite Y

Hyun Sung Kim, Nak Cheon Jeong, and Kyung Byung Yoon*

Contents

- SI-1. Local pH Variation in Zeolite-Y Depending on the Number of H^+ in A Unit Cell.
- S-2. Fabrication of the photovoltaic cells
- SI-3. Effect of ITO glass on the growth of zeolite films..
- SI-4. Diffuse-reflectance UV-vis spectra of $(2NH_4^+, CdS)_{6.3}Y_{ITO}$ after ODC coating, after exposure to air, and after immersion in the electrolyte solution
- SI-5. Stability of $(CdS)_{6.3}Y_{ITO}$ and $(PbS)_{6.7}Y_{ITO}$ after immersion in the electrolyte solution confirmed by X-ray diffraction intensities.
- SI-6. Stability of $(CdS)_{6.3}Y_{ITO}$ and $(PbS)_{6.7}Y_{ITO}$ after immersion in the electrolyte solution confirmed by AFM investigation of the surfaces.
- SI-7. Characterization of $(PbS)_{6.7}Y_{ITO}$ with transmission electron microscopy (TEM).
- SI-8. Transmittance spectra of $(Na)_{59}Y_{ITO}$ and $(CdS)_nY_{ITO}$ ($n = 3.2, 4.3, \text{ and } 6.3$)
- SI-9. Extrapolated plots of IPCE (A) and APCE (B) with respect to the loaded number of CdS per unit cell
- SI-10. Estimation of band gap energies of interconnected QDs in $(CdS)_{6.3}Y_{ITO}$ and $(PbS)_{6.7}Y_{ITO}$
- SI-11. Basis for the calculation of the volume percent of 6.3 CdS in a unit cell.
- SI-12. Calculation of the interdot distance between the interconnected CdS QDs in $(CdS)_{6.3}Y_{ITO}$.
- SI-13. Electrolyte salt occlusion into zeolite-Y films upon immersion into the electrolyte solution
- SI-14. Laser scanning confocal microscope (LSCM) images of the fluorescein-stained zeolite Y films
- SI-15 Photovoltaic characteristics of $(CdS)_{6.3}Y_{ITO} \mid Pt_{FTO}$ with various thickness.
- SI-16. Photovoltaic characteristics of $(CdS)_{6.3}Y_{ITO} \mid Pt_{FTO}$ under different light intensities.

SI-1. Local pH Variation in Zeolite-Y Depending on the Number of H⁺ in A Unit Cell.

Table SI-1. Local pH variation with changing the number of H⁺ ion in a unit cell.

$V_{UC} (m^3)^a$	N_{H^+}/V_{UC}^b	$N_{H^+}/1L^c$	$M_{H^+}^d$	pH
1.51×10^{-26}	1	6.64×10^{22}	0.110	0.958
	2	1.33×10^{23}	0.220	0.657
	3	1.99×10^{23}	0.330	0.481
	4	2.65×10^{23}	0.440	0.356
	5	3.32×10^{23}	0.551	0.259
	6	3.98×10^{23}	0.661	0.180
	7	4.65×10^{23}	0.771	0.113
	8	5.31×10^{23}	0.881	0.055
	9	5.97×10^{23}	0.991	0.004
	10	6.64×10^{23}	1.102	-0.042
	11	7.30×10^{23}	1.212	-0.084
	12	7.96×10^{23}	1.322	-0.121
	13	8.63×10^{23}	1.433	-0.156
	14	9.29×10^{23}	1.543	-0.188
	15	9.95×10^{23}	1.653	-0.218
	16	1.06×10^{24}	1.763	-0.246
	17	1.13×10^{24}	1.873	-0.273
	18	1.19×10^{24}	1.984	-0.297
	19	1.26×10^{24}	2.094	-0.321
	20	1.33×10^{24}	2.204	-0.343
	21	1.39×10^{24}	2.314	-0.364
	22	1.46×10^{24}	2.424	-0.385
	23	1.53×10^{24}	2.535	-0.404

^aVolume of a unit cell. ^bNumber of protons in unit cell volume. ^cNumber of protons in 1 L. ^dMolar concentration of proton.

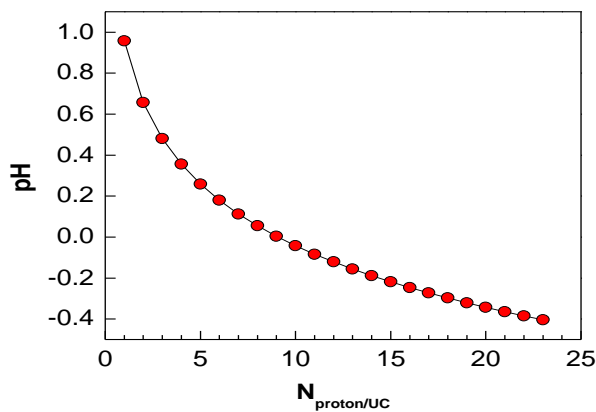


Figure SI-1-1. Plot of the calculated local pH with respect to the number of H⁺ ion in a unit cell of zeolite-Y.

S-2. Fabrication of the photovoltaic cells

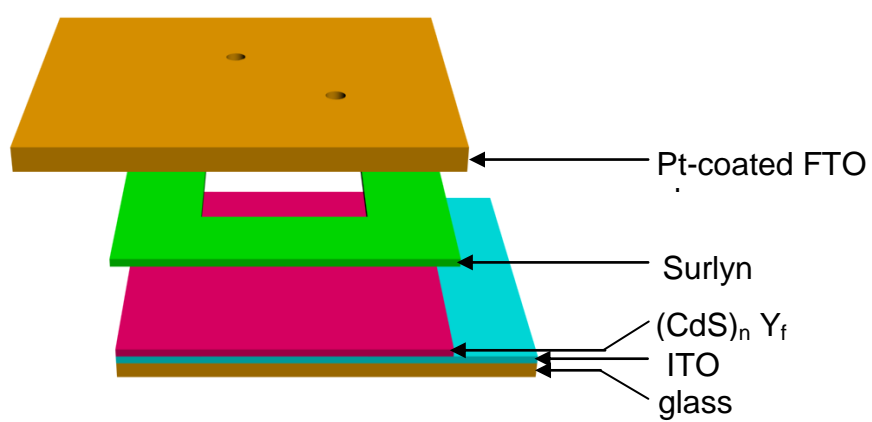


Figure SI-2-1. Schematic illustration of the components for the photovoltaic cell fabricated in this study.

SI-3. Effect of ITO glass on the growth of zeolite films..

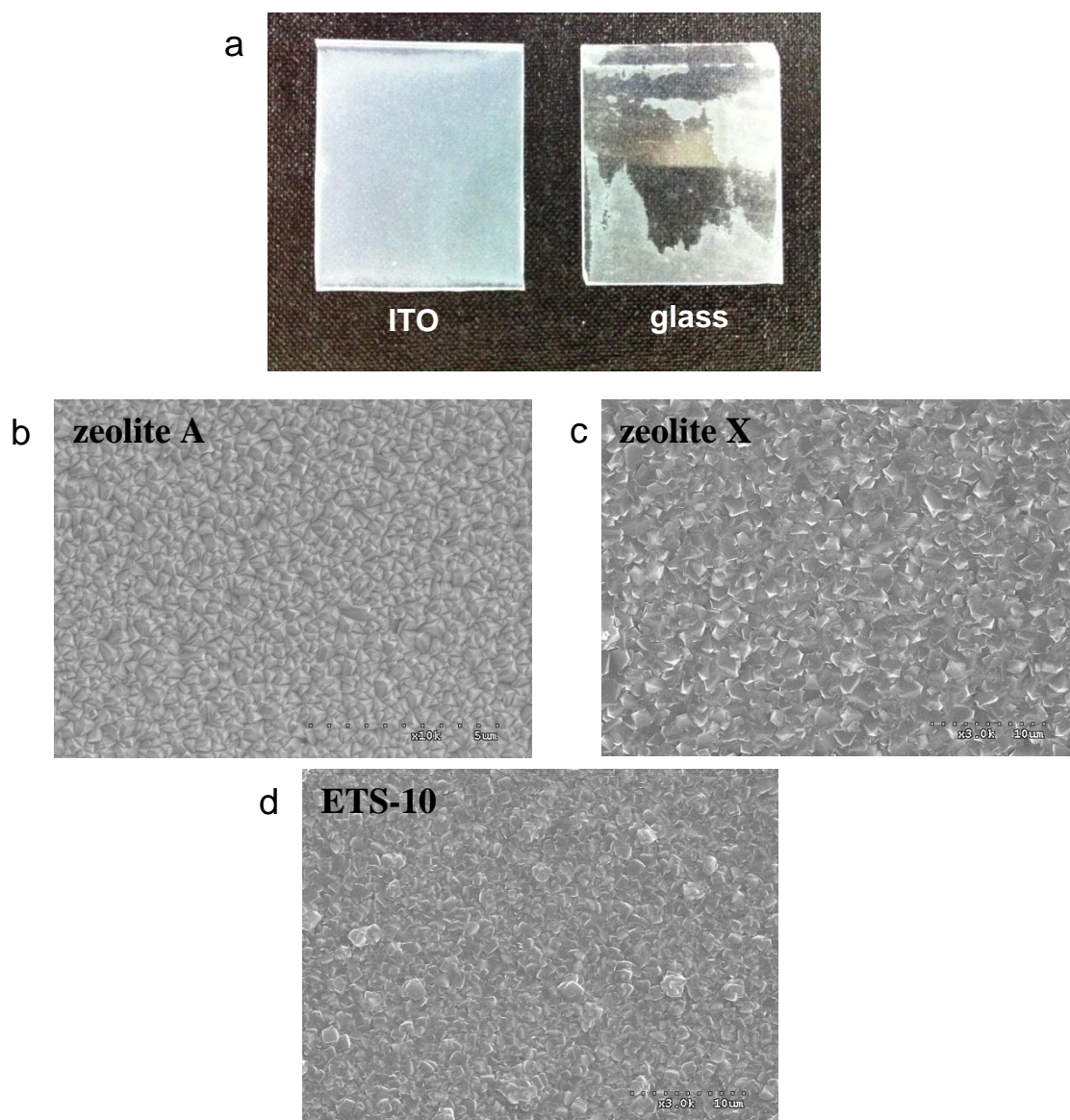


Figure SI-3-1. Photograph (a) and SEM images (b-d) showing the effect of ITO on the growth of zeolite films.

SI-4. Diffuse-reflectance UV-vis spectra of $(2\text{NH}_4^+, \text{CdS})_{6.3}\text{Y}_{\text{ITO}}$ after ODC coating, after exposure to air, and after immersion in the electrolyte solution

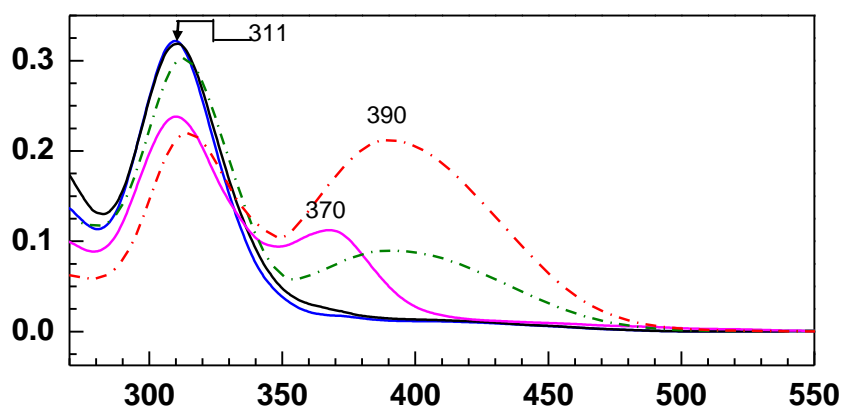


Figure SI-4-1. Diffuse-reflectance UV-vis spectra of $(2\text{NH}_4^+, \text{CdS})_{6.3}\text{Y}_{\text{ITO}}$ after three different types of treatment: ODC coating (black solid), after exposure to the atmosphere for 24 h (blue solid), and after immersion in the electrolyte solution for 12 h (pink solid), respectively. For comparison, the corresponding UV-vis spectra of $(2\text{H}^+, \text{CdS})_{6.3}\text{Y}_{\text{ITO}}$ after exposure to the atmosphere for 24 h (green dash dot) and after immersion in the electrolyte solution for 12 h (red dash and dot) are also shown.

SI-5. Stability of $(\text{CdS})_{6.3}\text{Y}_{\text{ITO}}$ and $(\text{PbS})_{6.7}\text{Y}_{\text{ITO}}$ after immersion in the electrolyte solution confirmed by X-ray diffraction intensities.

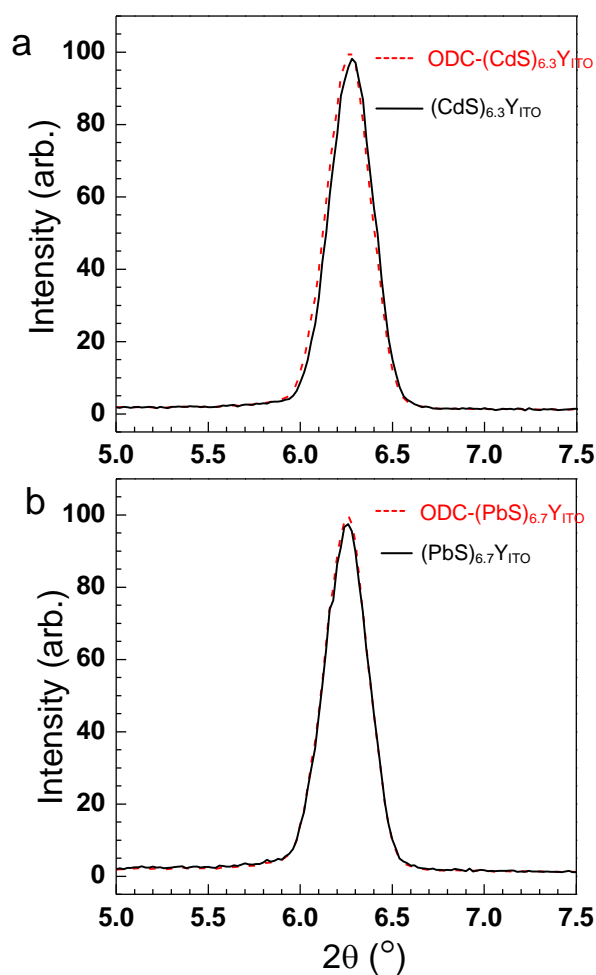


Figure SI-5-1. X-ray diffraction peaks at 6.25° arising from the diffraction by (111) plane of $(\text{CdS})_{6.3}\text{Y}_{\text{ITO}}$ (a) and $(\text{PbS})_{6.7}\text{Y}_{\text{ITO}}$ (b) after removal from the electrolyte solution for 12 h compared with those of the corresponding $\text{ODC}-(\text{CdS})_{6.3}\text{Y}_{\text{ITO}}$ (a) and $\text{ODC}-(\text{PbS})_{6.7}\text{Y}_{\text{ITO}}$ (b).

SI-6. Stability of $(\text{CdS})_{6.3}\text{Y}_{\text{ITO}}$ and $(\text{PbS})_{6.7}\text{Y}_{\text{ITO}}$ after immersion in the electrolyte solution confirmed by AFM investigation of the surfaces.

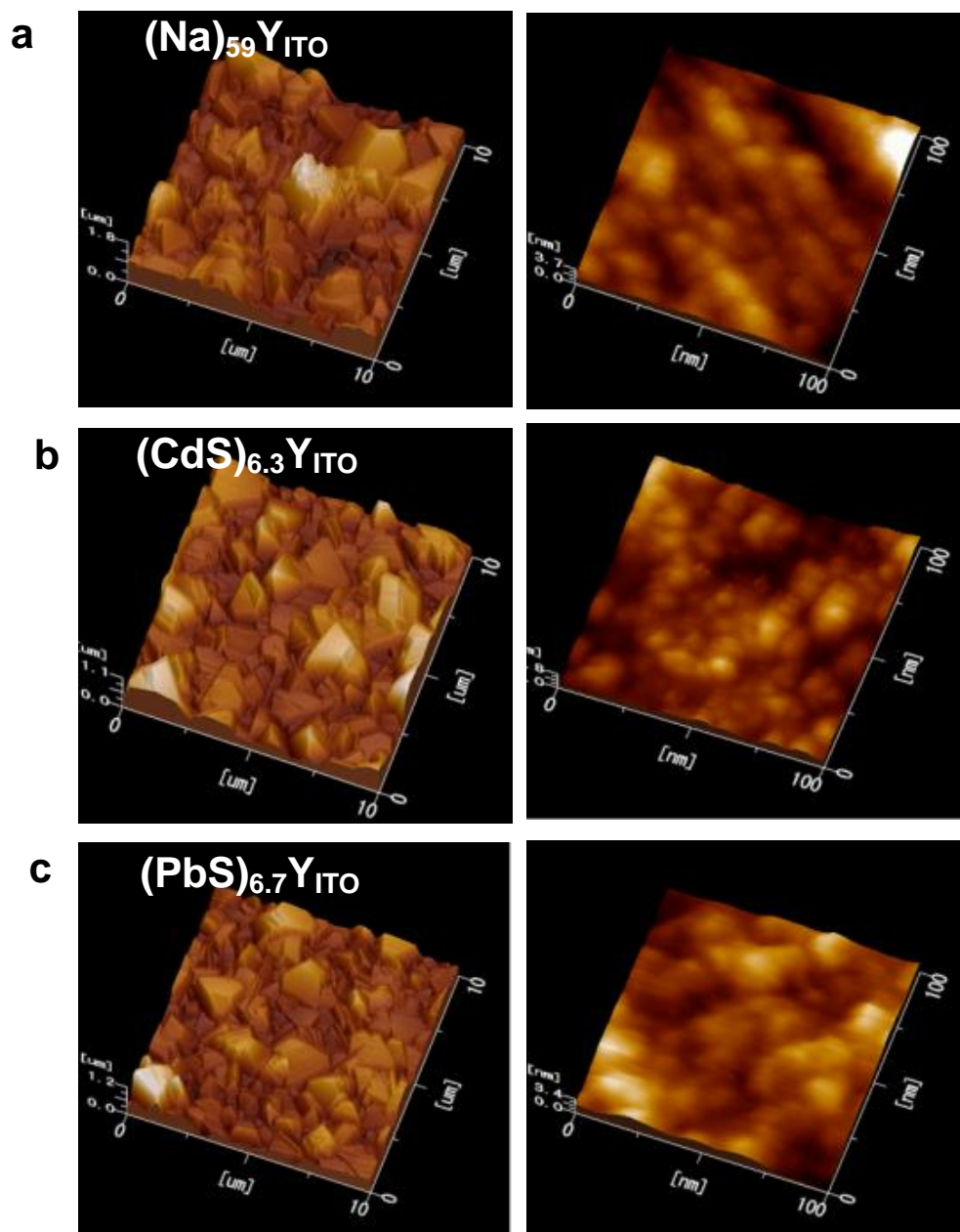


Figure SI-6-1. AFM images of $(\text{Na})_{59}\text{Y}_{\text{ITO}}$ (a), $(\text{CdS})_{6.3}\text{Y}_{\text{ITO}}$ (b), and $(\text{PbS})_{6.7}\text{Y}_{\text{ITO}}$ (c) in two different scales, $10 \times 10 \mu\text{m}^2$ (left) and $100 \times 100 \text{ nm}^2$ (right).

SI-7. Characterization of (PbS)_{6.7}Y_{ITO} with transmission electron microscopy (TEM).

For the TEM analysis, the (PbS)_{6.7}Y films were peeled off the ITO glass by scraping them with a razor blade in a glove box and the surfaces of the fragments were coated with ODC to preserve the QDs as such. The TEM images of the ODC-coated (PbS)_{6.7}Y film fragments showed only lattice fringes of zeolite Y framework but not the isolated QDs (Figure SI-7-1, a and b). However, the TEM images of the ODC-coated fragments of (PbS)_{6.7}Y film after immersion in the electrolyte solution for 12 h (Figure SI-7-1, c and d) show the presence of ~5 nm sized QDs on the surface, consistent with the observation of the exciton absorption in the diffuse reflectance UV-vis spectrum (Figure 2f in the text) and the globular PbS QDs observed by AFM (SI-6). The absence of the lattice fringes of the zeolite-Y framework on the surface further shows that the thin surface layers of (PbS)_{6.7}Y_{ITO} underwent framework decomposition during the formation of mesosized PbS QDs. In contrast to the surface, the internal areas of the (PbS)_{6.7}Y_{ITO} film remained intact (Figure SI-7-1, e) indicating that the structural decomposition accompanying the formation of PbS is limited to the very shallow (10-20 nm) surfaces of (PbS)_{6.7}Y_{ITO} film.

For comparison, we also obtained TEM images of ODC-coated 100-nm sized (PbS)_{6.7}Y crystals before (Figure SI-7-1, f and g) and after (Figure SI-7-1, h-j) exposure to the electrolyte solution for 12 h. The TEM images of ODC-coated (PbS)_{6.7}Y crystals, which were not exposed to the electrolyte solution, showed only the lattice fringes of the zeolite-Y framework but not the isolated PbS QDs. In contrast, the TEM images of ODC-coated (PbS)_{6.7}Y crystals which were exposed to the electrolyte solution showed the presence of mesosized PbS QDs in the entire mass and the zeolite Y framework has undergone complete framework destruction. This also shows that, for some unrevealed reasons, the (PbS)_{6.7}Y_{ITO} is much more stable in the electrolyte solution than the individual particles.

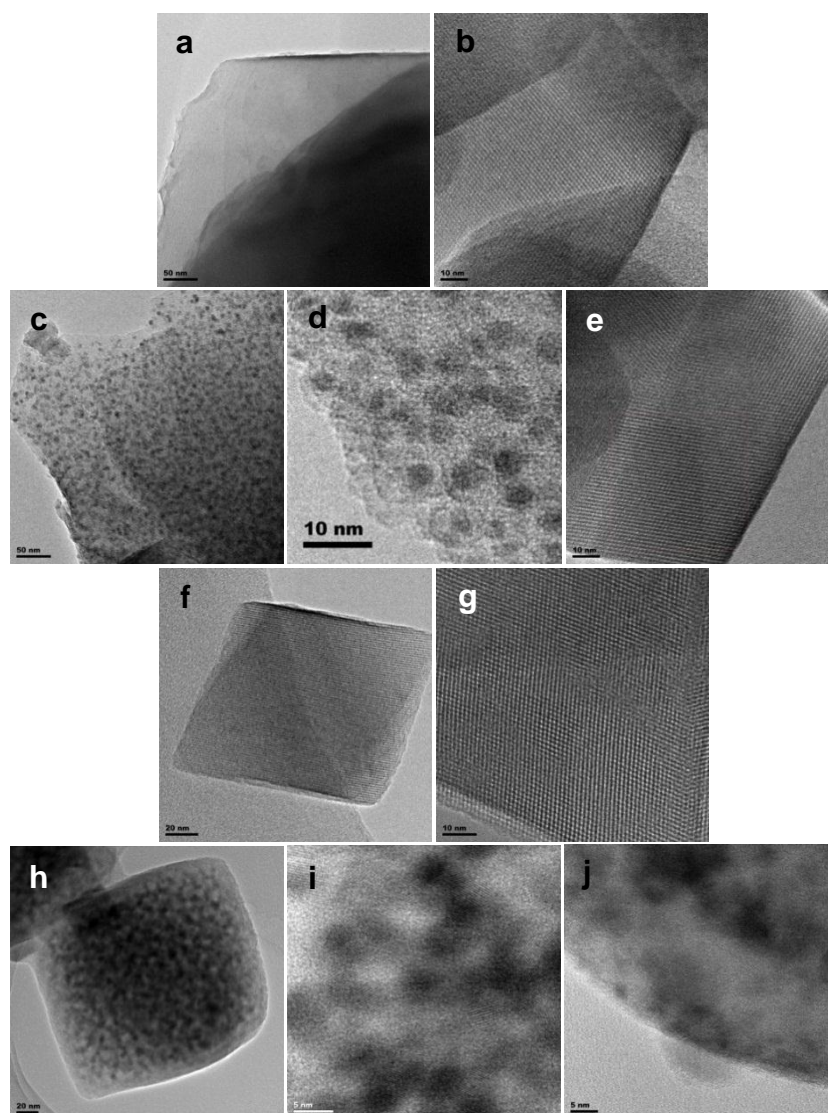


Figure SI-7-1. TEM images of zeolite films and zeolite crystals. $(\text{PbS})_{6.7}\text{Y}_{\text{ITO}}$ in different magnifications (a, b), a surface layer of $(\text{PbS})_{6.7}\text{Y}_{\text{ITO}}$ after immersion in the electrolyte solution for 12 h in two different magnifications (c, d), a deeper layer of $(\text{PbS})_{6.7}\text{Y}_{\text{ITO}}$ after immersion in the electrolyte solution for 12 h (e), 100-nm sized ODC- $(\text{PbS})_{6.7}\text{Y}$ crystals (f, g), 100-nm sized ODC- $(\text{PbS})_{6.7}\text{Y}$ crystals after immersion in the electrolyte solution for 12 h in different magnifications (h-j).

SI-8. Transmittance spectra of $(\text{Na})_{59}\text{Y}_{\text{ITO}}$ and $(\text{CdS})_n\text{Y}_{\text{ITO}}$ ($n = 3.2, 4.3$, and 6.3)

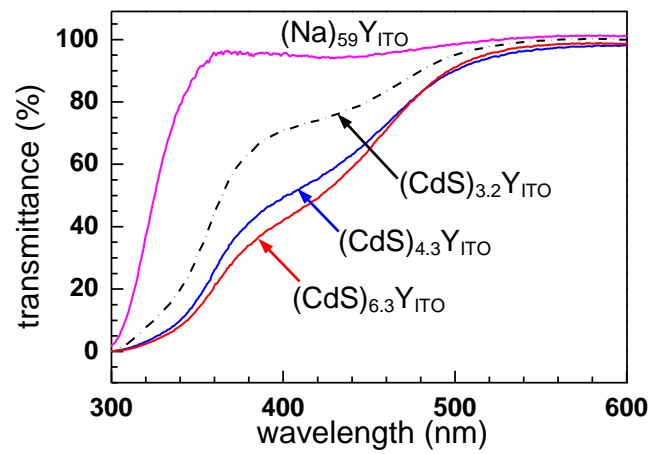


Figure SI-8. Transmittance spectra of $(\text{Na})_{59}\text{Y}_{\text{ITO}}$ and $(\text{CdS})_n\text{Y}_{\text{ITO}}$ ($n = 3.2, 4.3$, and 6.3) immersed in DMSO which is used as the index matching fluid.

SI-9. Extrapolated plots of IPCE (A) and APCE (B) with respect to the loaded number of CdS per unit cell

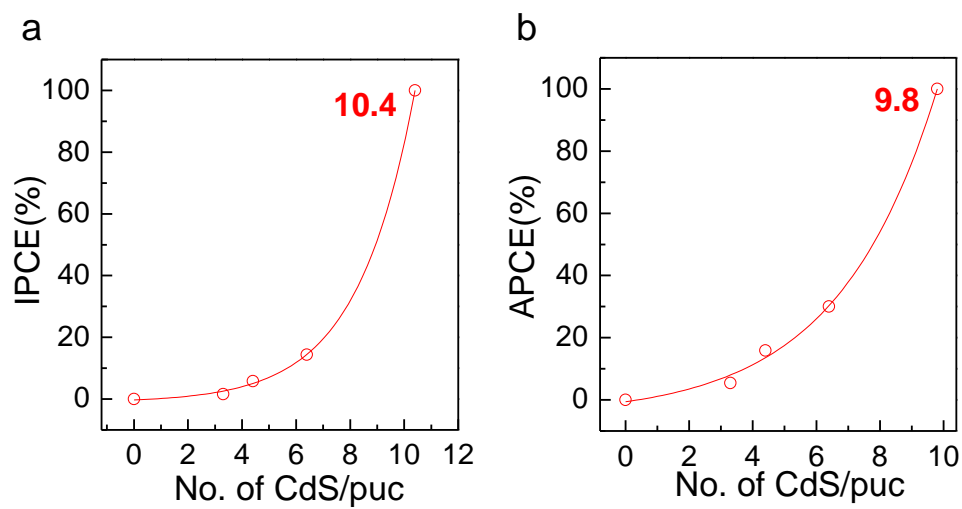


Figure SI-9-1. Plots of IPCE (a) and APCE (b) with respect to the loaded number of CdS per unit cell and the extrapolation.

SI-10. Estimation of band gap energies of interconnected QDs in $(\text{CdS})_{6.3}\text{Y}_{\text{ITO}}$ and $(\text{PbS})_{6.7}\text{Y}_{\text{ITO}}$

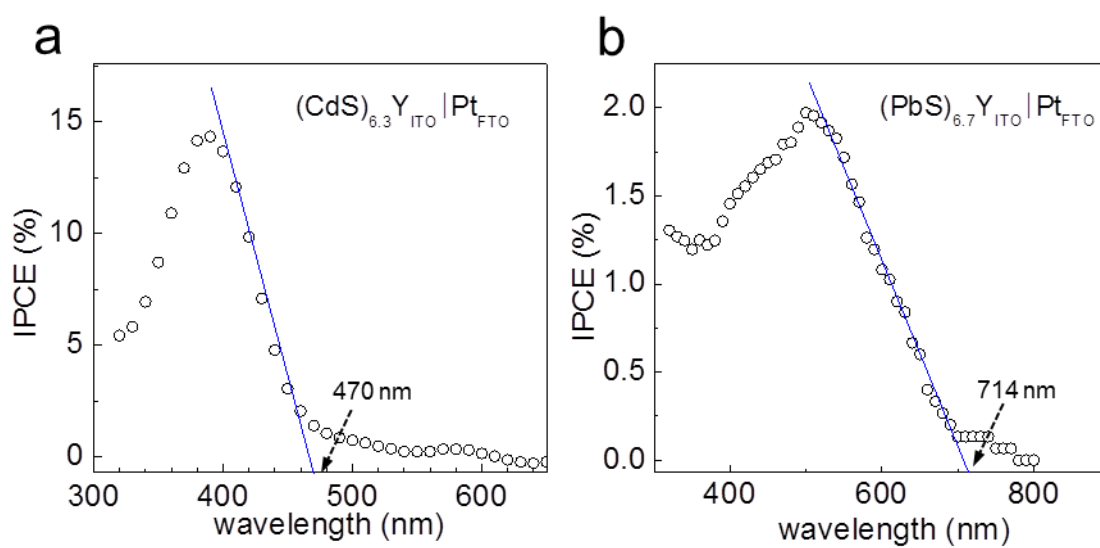


Figure SI-10-1. Estimation of band gap energies of interconnected QDs in $(\text{CdS})_{6.3}\text{Y}_{\text{ITO}}$ (a) and $(\text{PbS})_{6.7}\text{Y}_{\text{ITO}}$ (b).

SI-11. Basis for the calculation of the volume percent of 6.3 CdS in a unit cell.

(1) Number of CdS per unit cell = 6.3

(2) Density of CdS: 4.82 g/cm^3

(3) Molecular weight of CdS: 144.46 g/mole

(4) Weight of 6.3 CdS: $1.51 \times 10^{-21} \text{ g}$

(5) Volume of 6.3 CdS: 313 \AA^3

$$(1.51 \times 10^{-21} \text{ g})/V = 4.82 \text{ g/cm}^3$$

$$V = 313 \times 10^{-24} \text{ cm}^3 \quad (1 \text{ \AA}^3 = 10^{-24} \text{ cm}^3)$$

(6) Volume of a zeolite-Y unit cell: $14,349 \text{ \AA}^3$

(7) Volume % of 6.3 CdS in a unit cell: $(313/14,349) \times 100 = 2.2 \text{ (\%)}$

SI-12. Calculation of the interdot distance between the interconnected CdS QDs in $(\text{CdS})_{6.3}\text{Y}_{\text{ITO}}$.

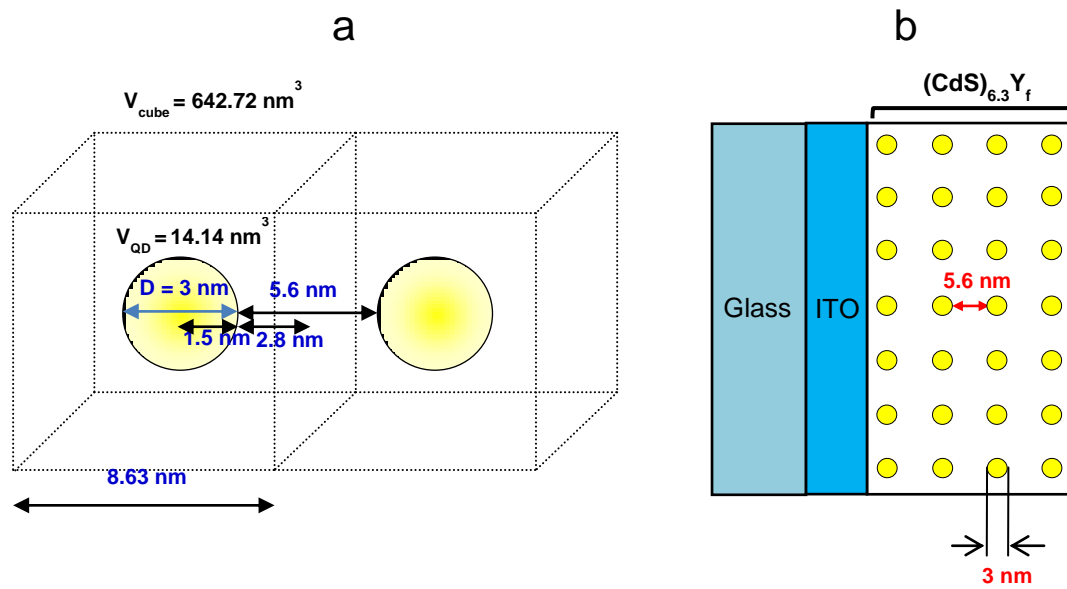


Figure SI-12-1. Schematic illustration of the basis for the calculation of the interdot distance between the interconnected CdS QDs in $(\text{Cd})_{6.3}\text{Y}_{\text{ITO}}$ (a) and the 2D drawing of $(\text{Cd})_{6.3}\text{Y}_{\text{ITO}}$ (B).

$D_{\text{QD}} (\text{nm})$	$r_{\text{QD}} (\text{nm})$	$V_{\text{QD}} (\text{nm}^3)$	$V_{\text{cube}} (\text{nm}^3)$	Edge length (nm)	Inter QD $d_{\text{edge-to-edge}}$
3.0	1.5	14.14	642.72	8.63	5.6

SI-13. Electrolyte salt occlusion into zeolite-Y films upon immersion into the electrolyte solution

Table SI-13-1. Compositions of Zeolite Y films After Immersion in Various Electrolytes Used in This Study.

Electrolytes	Unit Cell Composition + Additional Salt	
None	$\text{Na}_{70.2}\text{Al}_{70.3}\text{Si}_{121.7}\text{O}_{384}$	-
Na_2S (0.1M) + NaOH (1 M)	$\text{Na}_{70.2}\text{Al}_{70.3}\text{Si}_{121.7}\text{O}_{384} + (\text{Na}_{4.5}\text{S}_{0.7})$	0.1
Na_2S (0.1M)	$\text{Na}_{70.2}\text{Al}_{70.3}\text{Si}_{121.7}\text{O}_{384} + (\text{Na}_{0.5}\text{S}_{0.8})$	-
NaOH (1M)	$\text{Na}_{70.2}\text{Al}_{70.3}\text{Si}_{121.7}\text{O}_{384} + (\text{Na}_{3.8})$	-
NaI (0.1M) + NaOH (1 M)	$\text{Na}_{70.2}\text{Al}_{70.3}\text{Si}_{121.7}\text{O}_{384} + (\text{Na}_{4.6}\text{I}_{0.8})$	0.03
NaI (0.1M)	$\text{Na}_{70.2}\text{Al}_{70.3}\text{Si}_{121.7}\text{O}_{384} + (\text{Na}_{1.0}\text{I}_{0.9})$	-
TBAI (0.1M) + TBAOH (1 M)	$\text{Na}_{70.2}\text{Al}_{70.3}\text{Si}_{121.7}\text{O}_{384}$	0.0
TBAI (0.1M)	$\text{Na}_{70.2}\text{Al}_{70.3}\text{Si}_{121.7}\text{O}_{384}$	-

Procedure

1. Y_{ITO} films with the size of $2 \times 0.5 \text{ cm}^2$ were dipped into each electrolyte solution for 10 min.
2. Y_{ITO} films were washed with pure water for 3 second.
3. The surfaces were immediately dried by blowing strong N_2 flow.

SI-14. Laser scanning confocal microscope (LSCM) images of the fluorescein-stained zeolite Y films

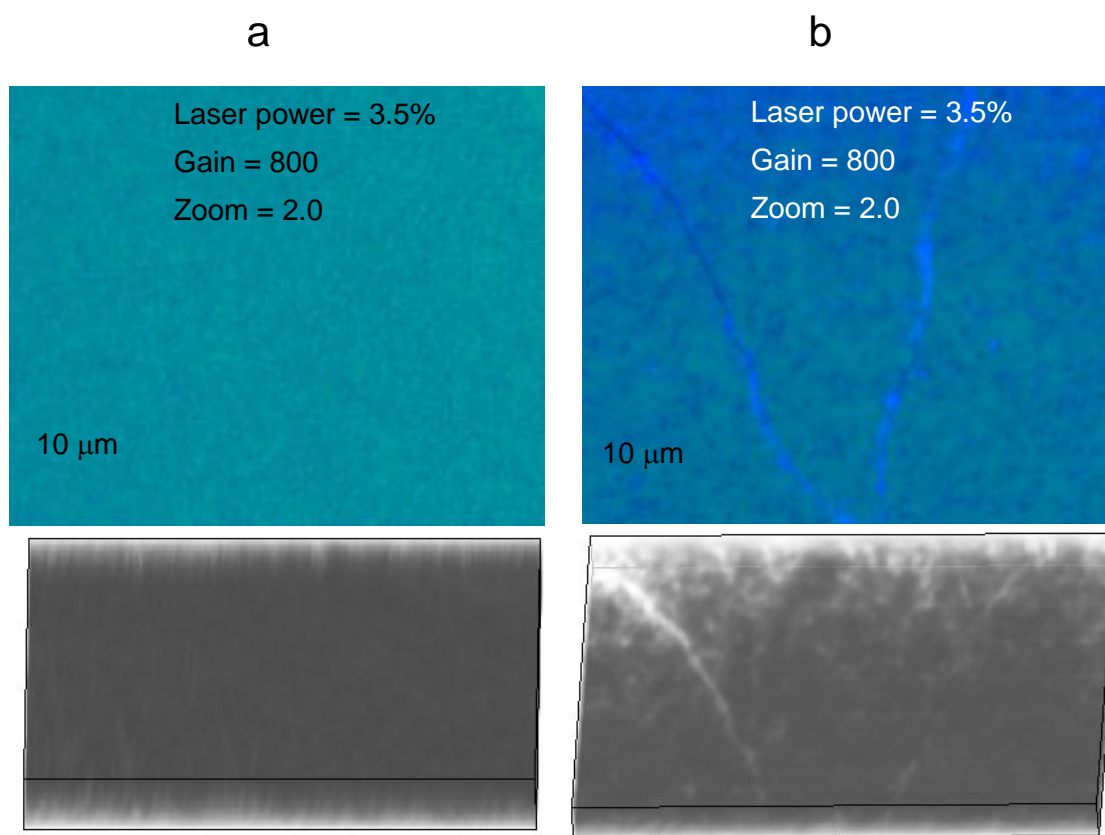


Figure SI-14-1. Comparison of two zeolite Y films: the one that is widely used in this study (a) and the other that has deliberately produced microcracks (b). Top: 2D image, Bottom: 3D image

The LSCM measurements were performed on two types of Y_{ITO} ($2 \times 2 \text{ cm}^2$), one that has been routinely used in this work, the other that have microcracks by generating large amounts of CdS QDs. The films were immersed in a methanol solution of 2-(6-hydroxy-3-oxo-(3H)-xanthen-9-yl) benzoic acid (fluorescein, 0.1M) for 4 days at room temperature. The zeolite-Y films were then washed with a stream of MeOH, dried by blowing N_2 gas, and kept at room temperature for 12 h.

The LSCM measurements were conducted using a LSM 5 Exciter (Carl Zeiss) with an Ar^+ ion laser (488 nm) as the excitation source and with z-stack scan mode. The two types of Y_{ITO} films were measured under the same condition of the laser power of 3.5 % using Plan-Apochromat 40 \times /0.95 Korr M27 objective lens with the zoom at 2.0 and the master gain at 800. The 3D images were built using ZEN 2009 Light Edition software (Carl Zeiss).

SI-15 Photovoltaic characteristics of $(\text{CdS})_{6.3}\text{Y}_{\text{ITO}} \mid \text{Pt}_{\text{FTO}}$ with various thickness.

\

Thickness (μm)	I_{sc} (mA/cm^2) ^a	V_{oc} (V) ^b	FF ^c	η (%) ^d
2500	0.30	423	28	0.10
1600	0.25	411	30	0.07
1000	0.17	397	28	0.04
500	0.10	384	29	0.02
350	0.07	350	30	~0.01

^aShort circuit current. ^bOpen circuit voltage. ^cFill factor. ^dEfficiency.

SI-16. Photovoltaic characteristics of (CdS)_{6.3}Y_{ITO} | Pt_{FTO} under different light intensities.

Light Intensity	I _{sc} (mA/cm ²) ^a	V _{oc} (V) ^b	FF ^c	η (%) ^d
1.0 sun	0.30	423	28	0.10
0.5 sun	0.18	415	30	0.13
0.1 sun	0.05	407	28	0.15

^aShort circuit current. ^bOpen circuit voltage. ^cFill factor. ^dEfficiency.